

# Homogeneous earth dam under seismic scrutiny: An evaluation study

# Comportamiento y vulnerabilidad sísmica de una presa de tierra homogénea

Camilo Marulanda<sup>1</sup>, William Ruíz<sup>2</sup>, David León<sup>3</sup>

- 1 Technical Manager, INGETEC, Bogotá, Colombia, marulanda@ingetec.com.co
- 2 Head of Dams Department, INGETEC, Bogotá, Colombia, wruiz@ingetec.com.co
- 3 PhD Student at Universitat Politècnica de Catalunya / Barcelona, Spain, david.eduardo.leon@upc.edu

ABSTRACT: The Quebradona dam is a 34 m high homogeneous earth dam built in the late 1950s. The original design of this dam did not include analyses to determine the stability conditions of the dam under seismic actions. Additionally, the Quebradona dam is founded on a thick residual soil that makes it susceptible to amplification and changes in frequency content of seismic motion. The updated seismic hazard study for this dam found that the verification seismic spectrum associated with the SEE (Safety Evaluation Earthquake) scenario for the Quebradona dam is characterized by an effective peak ground acceleration of 0.31 g. This paper will present the dynamic evaluation of the Quebradona Dam, including the collection and assessment of all information required for the analysis of the dam and its foundation, the engineering criteria for liquefaction potential and cyclic softening analyses, limit equilibrium analyses and numerical models. The purpose of the dynamic analysis performed was to evaluate the behavior and performance considering the recent seismic hazard study of 2021, reviewing the stability and vulnerability of the dam under the new conditions of the recommended Safety Evaluation Earthquake and the definition of the retrofitting works for the dam.

KEYWORDS: Dynamic behavior, earthquake, non-linear analysis, liquefaction, Quebradona Dam, Homogeneous embankment dam.

#### 1 INTRODUCTION

The Quebradona dam is a 34 m high homogeneous earth dam built in the late 1950s. The original design of this dam did not include analyses to determine the stability conditions of the dam under seismic actions. Additionally, the Quebradona dam is founded on a thick residual soil that makes it susceptible to amplification and changes in frequency content of seismic motion.

The updated seismic hazard study for this dam found that the verification seismic spectrum associated with the SEE (Safety Evaluation Earthquake) scenario for the Quebradona dam is characterized by an effective peak ground acceleration of 0.31 g. This value is 40% higher than that adopted in a previous assessment of the dam performed in 2006 where a value of 0.22g was used based on the design value of nearby the Río Grande II dam

With this background, the owner of the dam contracted the engineering services to carry out a seismic vulnerability study of the Quebradona dam. This paper will present the dynamic evaluation of Quebradona Dam, including the collection and assessment of all information required for the analysis of the dam and its foundation, the engineering criteria with which the liquefaction potential and cyclic softening analyses, limit equilibrium analyses and numerical models were developed. The purpose of the dynamic analysis performed was to evaluate the behavior and performance of this structure considering the results and conclusions of the recent seismic hazard study developed in the year 2021, reviewing the stability and vulnerability of the dam under the new conditions of the recommended Safety Evaluation Earthquake and the definition of the retrofitting works for the dam.

#### 1.1 Description of the dam

The Quebradona Dam, part of the Río Grande I Hydroelectric Project, is located 55 kilometers northeast of the city of Medellín (Colombia), between the municipalities of Don Matías and Santa Rosa de Osos. Figure 1 shows a plan view of the dam and the general location of the project.

Quebradona is a compacted earth dam with a height of 34 m from the lowest point of the foundation, the crest level is at EL. 2098 masl and the crest length is 110 m. The crest width is 8 m, free border equal to 3 m and it has a fill volume of approximately 331,000 m<sup>3</sup>. Figure 2 shows the maximum section of the dam.

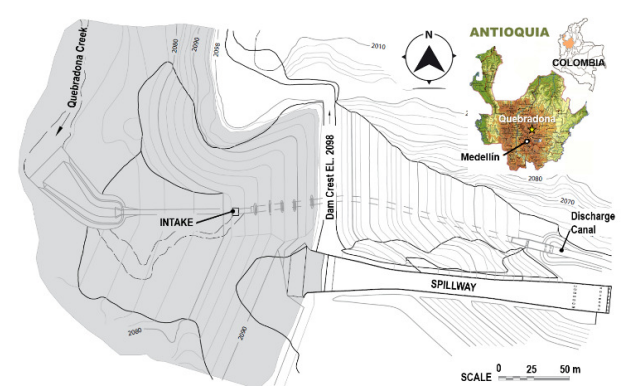


Figure 1. Localization and layout of the Quebradona dam.



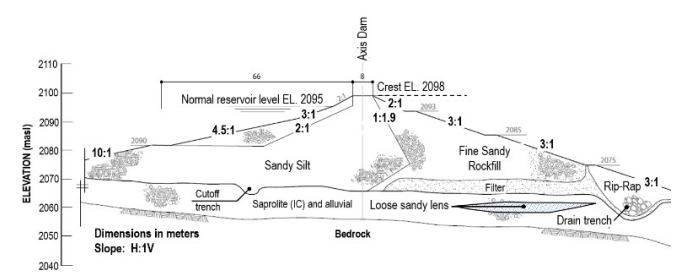


Figure 2. Maximum section of the Quebradona dam.

For the design of the Quebradona dam in 1955 no seismic criteria were considered, such as loss of free board due to settlement of the crest, evaluation of liquefaction, loss of shear strength of the body of the dam and its foundation, or design of protection elements to avoid internal erosion problems due to cracking of impermeable areas. The absence of seismic analysis and modern filter design criteria makes this study more relevant.

#### 2 SEISMIC HAZARD

A recent study (2021) that included a neotectonic evaluation seismic hazards analysis determined that for the Safety Evaluation Earthquake (SEE) for Quebradona Dam considers an effective peak acceleration of 0.27 g in rock. The study also established a spectral acceleration of 0.68 g on the dam platform (for periods shorter than the short period, or SDS) and a short period (T1) of 0.50 seconds. The analysis used the attenuation laws for crustal events of Abrahamson, Silva and Kamai (2014), Campbell and Bozorgnia (2014) and Chiou and Youngs (2014) proposed as part of the NGA-West 2 Project, and for subduction sources and Benioff the laws proposed by Atkinson and Boore (2003), Young et al., (1997) and Zhao et al., (2006).

Another scenario considered in the evaluation (Scenario 2) used the attenuation laws of the 2014 Western United States model (United State National Seismic Hazard Maps - US2014-NSHMP, Peterson et al. 2014), obtaining a Safety Evaluation Earthquake (SEE) for the Quebradona dam characterized by an Effective peak acceleration of 0.31 g, a spectral acceleration for periods less than T1 (SDS) of 0.77 g and a short period of 0.45 s. Figure 3 shows the verification spectra for the two scenarios analyzed in the aforementioned study.

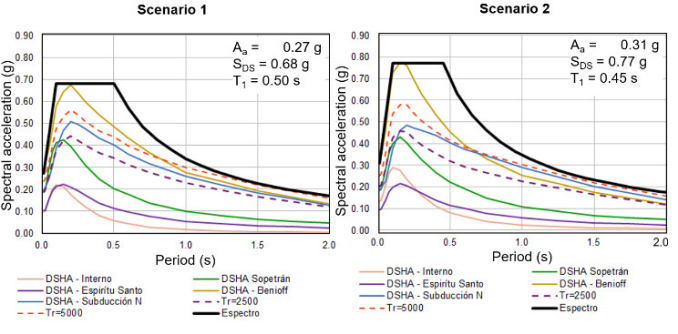


Figure 3. Seismic verification spectrum for the Safety Evaluation Earthquake (SEE) of Quebradona dam.

Figure 3 illustrates that the critical scenario with the highest acceleration was Scenario 2. For structural periods less than 1.0 s, the controlling event is an earthquake in the northern intermediate

Benioff zone, with a magnitude (Mw) of 7.8, an epicentral distance of 34 km, and a focal depth of 90 km. For periods greater than 1.0 s, the controlling event is an earthquake in the Northern Subduction Zone, with a magnitude (Mw) of 8.6, an epicentral distance of 166 km, and a focal depth of 40 km. In contrast, the cortical earthquake with the highest acceleration corresponds to the Sopetrán fault, part of the Romeral fault system, with a magnitude (Mw) of 6.7 and epicentral distance of 36 km.

Considering the previous control events, for the nonlinear dynamic analysis of the present study, five sets of ground motions were selected (each with two horizontal components and one vertical component) recorded in rock and generated by subduction and cortical earthquakes.

The subduction ground motions correspond to the Zihuatanejo and La Unión earthquakes, while the ground motions of the cortical earthquakes correspond to the San Fernando, Northridge and Iwate earthquakes, representative of the seismic hazard of the site and that when scaled present response spectra that fit the deterministic spectrum of the control events, as seen in Figure 4.

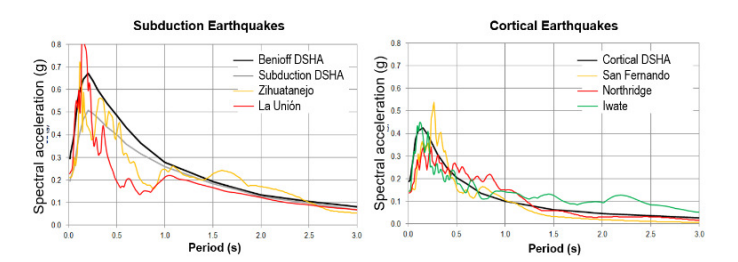


Figure 4. Comparison of response spectra of the selected ground motions and the deterministic spectra (DSHA) of the control events for the SEE.

# 3 MATERIAL PROPERTIES AND CONSTITUTIVE MODEL CALIBRATION

The development of the geotechnical model of the materials of embankment dam and its foundation, considered different geotechnical investigations developed at different moments of the project, including during the design stage of the project (1955) as well as subsequent studies executed in the 90's and in 2006 which included boreholes and installation of new geotechnical instrumentation. These explorations included SPT, seismic refraction lines, and drilling to recover undisturbed samples for laboratory shear strength testing. For the present study, new explorations consisting of seismic piezocone tests (sCPTu) were carried out.

The addition of piezocone tests aimed to enhance the characterization of the dam materials and to assess the extent of a loosely packed sandy lens discovered in 2006. This feature raised concerns about potential liquefaction risks during seismic events.

The shear strength parameters under drained conditions of the different materials of the dam body and foundation were estimated using empirical correlations from SPT and sCPTu tests, and the results of CU triaxial testing on undisturbed samples.

The geotechnical model considered seven material types, four for the embankment dam and three for the foundation, as shown in Figure 5 and Table 1.



Table 1.	Geotechnical zoning, average shear strength parameters,
permeab	ility, and constitutive models for numerical analyzes.

ID	Material	γ	c'	φ'	Constitut.	k	
ш	Matchai	$(kN/m^3)$	(kPa)	(°)	Model	(m/s)	
	Sandy silt	19.6	4 - 14	30	2D: PM4Silt	1.3x10 <sup>-7</sup>	
	Salidy Silt		4 - 14 30		3D: P2P Sand	1.5X10	
H	Sandy	19.8	5 20	36	2D: PM4Silt	£ 010.7	
Dam	rockfill		5 - 20		3D: P2P Sand	5.8x10 <sup>-7</sup>	
	Filter	19.5	0	35	MC	1.8x10 <sup>-3</sup>	
	Rip-Rap	20.0	0	40	MC	1.0x10 <sup>-2</sup>	
	Residual	17.8	42	29	2D: PM4Sand	1.5x10 <sup>-6</sup>	
	Soil (IB)		42		3D: P2P Sand	1.5X10 °	
Found	Saprolite	18.9	40	49 30	2D: PM4Sand	<b>5.5.10</b> -7	
	(IC)		49		3D: P2P Sand	7.5x10 <sup>-7</sup>	
	Loose	16.0		0 24	2D: PM4Sand	20.10-4	
	sandy lens		0		3D: P2P Sand	2.9x10 <sup>-4</sup>	

The undrained shear strength for the sandy silt and fill material of the embankment dam was obtained in terms of the ratio  $Su/\sigma$ 'v estimated based on correlation with the CPTu and SPT and the results of the undrained triaxial test.

Sandy Silt 
$$\Rightarrow Su / \sigma'_v = 4,6 (\sigma'_v)^{-0.42}$$
 (1)  
Sandy fill  $\Rightarrow Su / \sigma'_v = 5,0 (\sigma'_v)^{-0.41}$  (2)

An expression considering the maximum shear modulus variation with the confinement was adjusted from the shear wave velocity measured of the MASW and SCPTu test, and the correlation of Robertson (2015) using the CPTu results. This value was used as a starting point in the numerical simulation and was then adjusted to match the fundamental period of the dam.

$$G_{max} = 1150 \, p_{atm} \, (p'/p_{atm})^{0.5}$$
 (3)

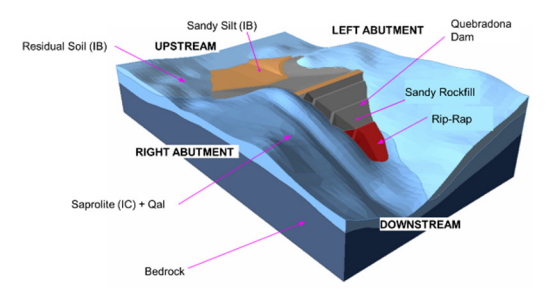


Figure 5. Geotechnical model and material for embankment dam and foundation.

The constitutive models for each material of static and dynamic analysis are described below, as well as parameter calibration.

#### 3.1 Mohr-Coulomb with hysteretic damping

This model was used for the filter and Rip-Rap at the toe of the dam, where deformation softening behavior is not expected and the important behavior to capture is shear resistance and damping.

Figure 6 shows the best fit of the 'default' model for the reference curve of these materials, corresponding to the average curve of Seed and Idriss (1970) for sands, and a good fit of the model is seen with the parameters L1 and L2 of -3.32 and 0.823, respectively.

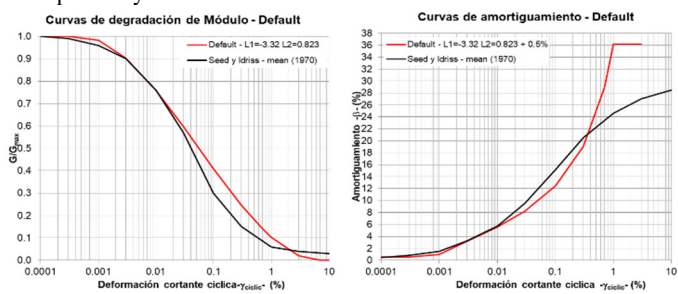


Figure 6. Shear modulus reduction and damping ratio for granular material - Default model.

#### 3.2 PM4sand

This model was used to simulate the behavior of the mainly granular materials of the two-dimensional model, the loose alluvial sand and the IC weathering profile of the foundation.

The relative density was defined based on the results of the SPT and SCPTu in situ tests, while the parameter  $G_0$  corresponds to the value obtained from the calibration of the fundamental period of the three-dimensional model. Additionally, the ratio of plastic modulus to elastic modulus  $h_0$  and some secondary parameters were calibrated simulating elemental cyclic simple direct shear tests and adjusting the modulus and damping degradation curves and reference cyclic resistance, which for the case of the weathering profile IC corresponds to the Darendeli curve with IP=8% and the cyclic resistance curve obtained from triaxial tests.

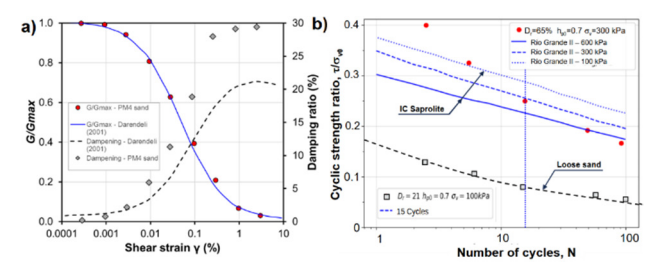


Figure 7. Model PM4Sand- IC Foundation and loose sandy lens a)
Shear modulus and damping ratio degradation curve adjustment and b)
Cyclic resistance curve.

As presented in Figure 7a and Figure 7b, with the calibration carried out to the parameters of the PM4Sand model, a satisfactory fit was achieved both of the reference cyclic resistance curve, considering liquefaction when a shear strain of 3% is reached, and of the modulus and damping degradation curves. As shown in Figure 7a, the calibrated model predicts higher damping at large strain than the reference curve. Boulanger and Ziotopoulou (2017) identified this as a limitation of the model and therefore does not correspond to a parameter calibration problem.

The summary of calibrated parameters of the PM4Sand model for the IC foundation profile and loose alluvial sand is presented in Table 2. Due to the unavailability of reference cyclic resistance curves for loose sand, the model's default secondary parameters and a contraction rate parameter (h<sub>p0</sub>) of 0.7 were used. This



produces an adequate fit to the Idriss and Boulanger's (2008) resistance curve liquefaction for a  $(N_1)_{60}$  of 2. In other words, for a cyclic stress ratio of 0.08, liquefaction occurs for approximately 15 uniform load cycles.

Table 2. PM4Sand model parameters – IC foundation and loose sand.

Parameter	Saprolite IC	Loose alluvial sand	
$D_r$	0.65	0.21	
$G_0$	1400	1000	
$h_{p0}$	0.70	0.70	
$h_0 = (0.25 + D_r)/2$	0.70		
Critical State: $Q = 10$	10.70	Default values of the	
Critical State: $R = 1$	1.40	model were used	
$C_{GD}=2$	8.00		

#### 3.3 PM4Silt

This constitutive model is suitable for simulating the behavior of intermediate materials between sands and clays, so it was used in the simulation of the dam body materials in the two-dimensional finite difference model. The basic parameters of the model corresponding to the undrained shear strength  $(S_u/\sigma'_v)$  and the variation of the maximum shear modulus  $(G_0$  and  $n_G)$  were defined from the geotechnical characterization and the calibration process of the fundamental frequency of the three-dimensional model. On the other hand, the contraction rate parameter  $(h_{p0})$  and some of the secondary parameters of the model were calibrated from the simulation of cyclic simple direct shear tests and the calibration of the reference modulus and cyclic strength degradation curves.

Figure 8a and Figure 8b show the adjustment made to the shear modulus and damping ratio degradation curve for the dam's body and the cyclic resistance curve, respectively. These curves were obtained by simulating different cyclic simple shear tests under undrained condition both for different uniform cyclic stress ratios and controlled strain.

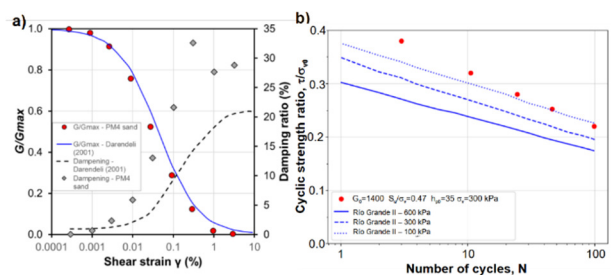


Figure 8. Model PM4Silt - embankment dam (sandy silt and fine sandy rockfill). a) Shear modulus reduction and damping ratio and b)

Cyclic resistance curve adjustment.

As seen in these figures, the calibration carried out to the model parameters achieved adequate adjustment of these curves, except for the damping for shear deformations greater than 0.1% due to the same limitation that the PM4Sand model presents. Table 3 summarizes the calibrated parameters of the PM4Silt model for embankment dam materials (sandy silt and fine sandy rockfill).

Table 3. PM4Silt model parameters – Embankment dam (sandy silt and fine sandy rockfill).

Parameter	Sandy silt	Sandy rockfill
$S_u/\sigma'_v$	$4.6 (\sigma'_{v})^{-0.42}$	$5.0 (\sigma'_{v})^{-0.41}$
$G_0$	1400	1400

Parameter	Sandy silt	Sandy rockfill	
$h_{p0}$	35	35	
$n_G = 0.75$	0.50	0.50	
$h_0 = 0.5$	0.75	0.75	
$e_0 = 0.9$	0.65	0.65	
e-ln(p'): $\lambda = 0.06$	0.07	0.07	
$\phi'_{CS} = 32$	The default values of the model were used		
$n^{bwet} = 0.8$	1.0	1.0	
$n^{bdry}=0,5$	0.2	0.2	
$c_z = 100$	200	200	
$C_{GD} = 3$	15.0	15.0	

#### 3.4 P2PSand

This model developed primarily for granular materials, was used in the three-dimensional model to approximate the material response of the dam body and foundation. Calibration was done similarly to the previous models, simulating cyclic simple direct shear tests in undrained condition to adjust the modulus and damping degradation curves and the cyclic resistance curve.

Figure 9 shows the fit made to the reference curves of soil foundation, where it is observed that a good fit was obtained for the shear modulus and damping degradation curve, even for deformations greater than 0.1%, but with a point at 3x10<sup>-3</sup>%, where there is a jump in behavior compared to the other data. This value is due to the transition between elastic behavior (within the yield surface) and plastic behavior.

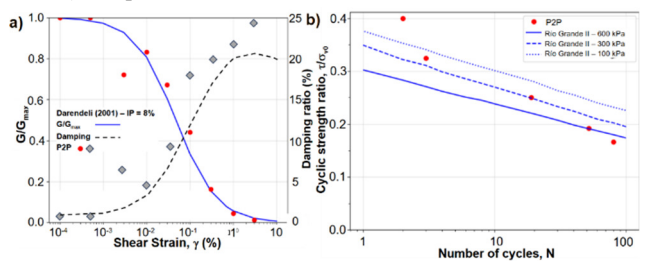


Figure 9. a) Shear modulus reduction, damping ratio and b) cyclic resistance curve adjustment - Model P2PSand - Soil Foundation.

The cyclic resistance curve of Figure 9 shows a good fit of the reference curve of Río Grande II project for a confinement of 300 kPa, corresponding to the average confinement of soil foundation in the maximum section of the dam and the confinement of the simple direct shear tests used for model calibration.

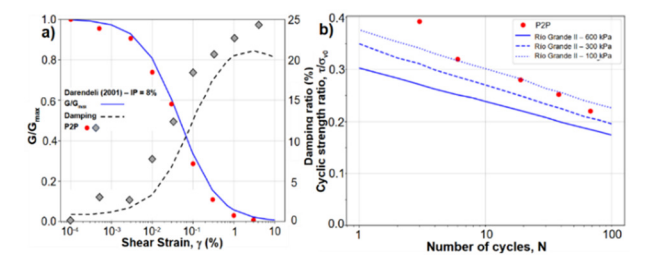


Figure 10. a) Shear modulus reduction, damping ratio and b) cyclic resistance curve adjustment - Model P2PSand – Embankment Dam.

Figure 10 shows the results of the adjustment made to the reference curves for shear modulus, damping ratio and cyclic



resistance for the materials of the dam body (sandy silt and decomposed rock). Although the P2PSand model is developed mainly for granular materials.

Figure 10 shows a good fit of this model for the dam body, achieved by adjusting the parameters that control the plastic volumetric deformation, such as the plastic volumetric rate A<sub>0</sub>, adjusted based on laboratory test values.

Table 4 presents the summary of the calibrated parameters of the P2PSand model for the foundation materials and the dam body. In the case of loose sand, only the initial relative density and the shear modulus coefficient were defined, according to the results of the field tests, while the other parameters correspond to the default values defined by Cheng and Detournay (2021).

#### 4 GEOTECHNICAL ANALYSES

#### 4.1 Liquefaction potential and cyclic softening analyses

Susceptibility to liquefaction was initially evaluated with the Bray and Sancio (2006) criterion, using index properties of the materials. The sandy silt and sandy rockfill that make up the body of the dam have moisture contents less than 80% of the liquid limit, which does not make them susceptible to liquefaction processes. These low moisture contents result of the low humidity during the construction and compaction processes of these materials.

Regarding the IB and IC weathering profiles of the foundation, slightly higher w<sub>n</sub>/LL ratios are observed than those of the dam body materials. However, most data show moderate susceptibility. The difference between the results of the foundation soil and the materials of the dam body is mainly due to the low moisture content and the higher dry densities with which the latter were built, since in terms of plasticity the materials are equivalent.

Table 4. P2PSand model parameters – Embankment dam and soil foundation

Parameter	Fill Dam	Foundation - IC	Loose Sand
$D_{r0}$	0.57	0.65	0.21
$G_r$	1400	1600	1000
(Q,R) = (10,1)	а	A	а
$h_0 = 1,7$	2.0	2.0	а
$n^b = 0.16 - \phi_{cs}/400$	a	a	а
$n^d = 6 n^d$	0.31	0.31	а
$A_{d0} = f(M^b - M^d)$	0.10	0.15	а
$z_{max} = min(21D_r^{3.85}, 15)$	15	15	а
$c_z = G_r$	1400	1600	а
$K_c = 3.8 - 7.2D_{r0} + 3.0D_{r0}^2$	0.11	0.22	а
$k_d = 0.46 - 0.35D_{r0}$	0.35	0.33	а

The evaluation of the potential for liquefaction and cyclic softening of the materials of dam and its foundation was assessed using different methodologies based on the number of blows of the SPT, the tip resistance of the piezocone test and the shear wave speed Vs measured in the MASW and sCPTu geophysical tests.

Figure 11 shows the results of this evaluation for the explorations in the central area of the dam, in the material corresponding to the sandy silt. As seen in this figure, the FS obtained from the SPT blow count is generally less than 1.0, indicating the possibility of liquefaction in this material. These

results are contrary to those obtained through the shear wave velocity with the methodology of Kayen et al (2013) where only a few points have a safety factor less than 1.0.

Regarding the results with the tip resistance of the sCPTu, the two methodologies analyzed present completely different results, with average FS of 0.5 according to Boulanger and Idriss (2014) and FS greater than 1.5 according to the methodology of Robertson (2009). The differences in these results are due to the fact that the methodology of Boulanger and Idriss (2014) considers that the material analyzed is a sand with non-plastic fines, while the methodology of Robertson (2009) divides the evaluation of liquefaction potential according to the type of material behavior (SBT<sub>n</sub>), evaluating materials with sand behavior based on the equivalent penetration resistance for a clean sand (Qtncs) in a similar way to the methodology of Boulanger and Idriss, while in materials with behavior of fine material, cyclic softening is evaluated from the undrained shear resistance, the latter being the type of behavior evidenced in the piezocone explorations carried out in this study.

The results of the evaluation of the liquefaction and softening potential in the downstream embankment formed by the sandy rockfill showed a behavior like those of the silty sand, where the methodology of Boulanger and Idriss (2014) for the SPT and the tip resistance of the sCPTu indicated safety factors against liquefaction less than 1.0, while the Robertson (2009) methodology showed FS greater than 1.5. This difference originates because the sandy rockfill of downstream embankment is a silty sand with a significant content of fines, which dominate the behavior of the material. Therefore, Robertson's (2009) methodology is the most appropriate to evaluate the liquefaction and cyclic softening potential of this type of materials.

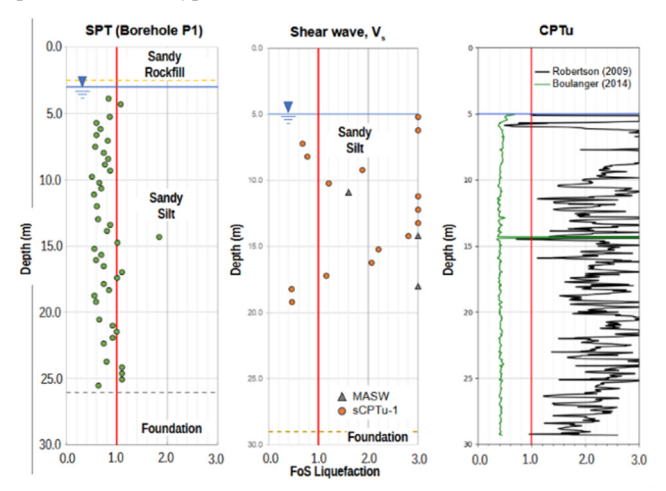


Figure 11. Results of liquefaction evaluation near the dam crest.

Finally, the results obtained in the loose alluvial sand stratum identified in the foundation, where SPT values between 2 and 6 blows/foot were recorded, for the methodology of Boulanger and Idriss (2014) report safety factors against liquefaction of less than 0.3, which makes it highly probable that liquefaction will occur in this material under the event of the safety verification earthquake (SEE) with a PGA of 0.31 g.



Proceedings of the 17<sup>th</sup> Pan-American Conference on Soil Mechanics and Geotechnical Engineering (XVII PCSMGE), and 2<sup>nd</sup> Latin-American Regional Conference of the International Association for Engineering Geology and the Environment (IAEG), La Serena Chile, 2024.

#### 4.2 Seepage analyses

#### 4.2.1 Two-dimensional model

The two-dimensional flow model was developed in Rocscience's Slide software using initial permeabilities estimated from in situ tests. Due to the very high pore pressures identified in the downstream shell associated with an insufficient capacity of the drain blanket and with the contribution of subsurface flow from the left abutment, it was not possible to obtain a calibration of the permeabilities that satisfied both the pore pressures in the body of the dam and the infiltration flows.

The total hydraulic gradients and leakage at the foot of the dam with the reservoir at the maximum level are presented in Figure 12, where it can be seen that towards upstream the flow lines present a very important vertical component, leading them towards the foundation and the filter of the dam where the flow is mainly horizontal. Therefore, the greatest gradients occur upstream between the contact of the sandy silt with the shell and the foundation. Furthermore, towards the foot of the dam, where the greatest internal erosion problems generally occur, there are total hydraulic gradients of 0.20, which are lower than the admissible hydraulic gradients for this material (0.25 for gravel).

The flow components at the contact of the sandy rockfill and the drain blanket are mainly horizontal, so the hydraulic gradients in this area have values below 0.25, which is less than admissible hydraulic gradient for this material. Regarding the leakages, the seepage analyzes showed a unit value of 0.0593 l/s/m, which with an equivalent width of dam equal to 58 m, represents an infiltration flow of 3.4 l/s, which is within the values measured by the V-notch sharp-crested weir installed at the foot of the dam when the reservoir level is in the vicinity of the EL. 2095 masl and is very similar to the infiltration flow estimated in the dam design (Gannet Fleming Corddry & Carpenter, Inc and Integral, 1958).

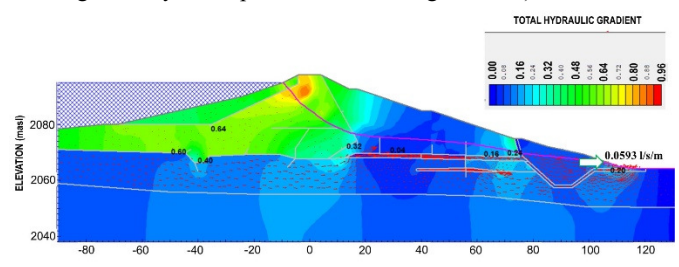
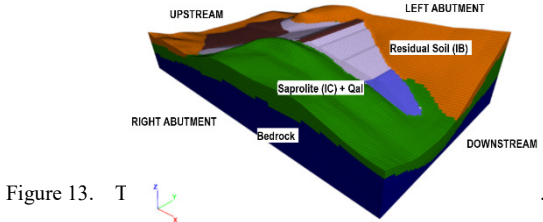


Figure 12. 2D seepage analysis with reservoir at operation maximum level - Hydraulic gradients.

## 4.2.2 Three-dimensional model

The three-dimensional flow model was developed using FLAC3D with the finite difference mesh presented in Figure 13, which considers the real geometry of the abutments and includes the IB weathering profile in the left abutment. Because the results of this flow analysis were used as the initial pore pressure field for the nonlinear dynamic analyses, the calibration was based primarily on obtaining pore pressures in the body of the dam that adequately represent the real conditions when the reservoir is at the operation maximum level.



The pore pressure field obtained from the 3D flow analysis with the reservoir at its maximum level over the maximum section of the dam with the location of some of the piezometers is presented in Figure 14. This figure shows a good fit of the piezometers located in the sandy silt such as PH5, PH11 and PH12 and an adequate fit, but with greater differences towards downstream, such as the piezometers PA3, PN5 and PA4 where the model records slightly lower pore pressures.

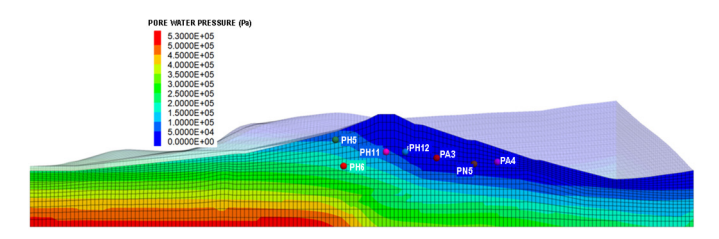


Figure 14. 3D seepage analysis with reservoir at operation maximum level – Water Pore Pressure.

#### 4.3 Slope stability analysis by limit equilibrium

#### 4.3.1 Two-dimensional analysis

The 2D stability analyzes were developed with the generalized limit equilibrium method (GELM) with slices from the maximum section of the dam, considering the pore pressures obtained from the seepage analyzes and the average shear strength of the materials. In addition, sensitivity analysis was also carried out with the lower and upper limits of the cohesion and friction of the materials, to establish the range of variation of the safety factor.

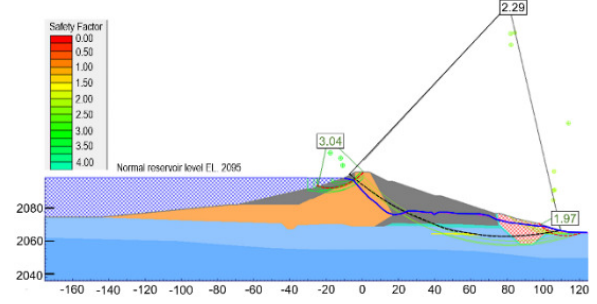


Figure 15. 2D stability analysis results - Static condition with reservoir at maximum level.

The stability results for the steady state flow condition with reservoir at EL. 2095 masl (Max. Level) and the average shear strength parameters are presented in Figure 16. Table 5 presents the results of the safety factor for the rest of the scenarios, together with the three-dimensional analyzes and the percentage change. These results show safety factors greater than 2.00 in static condition, 1.30 in case of rapid drawdown and greater than 1.00



under pseudo-static condition, which are above of the minimum safety factor recommended for embankment dams according to USACE (2003). The authors, the criterion of recommendation of a safety factor for a pseudo-static for evaluating this type of structure is not adequate, and the general recommendation for a dam should be rather a deformation criterion (Marulanda et al, 2023).

Table 5. Summary of safety factors from slope stability analyzes of Quebradona dam in two and three dimensions.

Scenario	Shoulder	Safety Factor		
Scenario		2D	3D	%Change
Static at Max.	Upstream	3.04	2.92	-4%
Reservoir Level	Downstream	2.29	2.74	+20%
Rapid drawdown up EL. 2080.13 masl	Upstream	1.37	1	
Pseudo-static	Upstream	1.77	1.46	-18%
$K_h = 0.16 g$	Downstream	1.42	1.74	+23%
Pseudo-static	Upstream	1.50	1.24	-17%
$K_h = 0.21 g$	Downstream	1.27	1.50	+20%

#### 4.3.2 Three-dimensional analysis

The three-dimensional stability analyzes were developed in Rocscience's Slide3 software using the geometry presented in Figure 5 and considering the pore pressures through a phreatic surface, which was constructed from the three-dimensional seepage analyzes presented in the previous section. These analyzes were carried out for the static and pseudo-static condition with the reservoir level in the NAMO. Not rapid drawdown condition was analyzed.

The stability results for the static condition are presented in Figure 16, where the global minimum failure surface on the downstream embankment develops from the crest of the dam to the berm of the EL. 2085 masl and presents a safety factor of 2.74, which is 20% higher than that obtained in the two-dimensional model.

The results of the limit equilibrium stability analyzes indicate that in general the safety factors obtained for the downstream embankment in the three-dimensional model are between 4% and 26% higher compared to the 2D results, showing an important three-dimensional effect due to the narrow canyon and the slight curve of this shoulder at the level of the rip-rap, which restricts the depth of slip surfaces identified in the two-dimensional analyzes that extend through the foundation and the loose alluvial sand stratum.

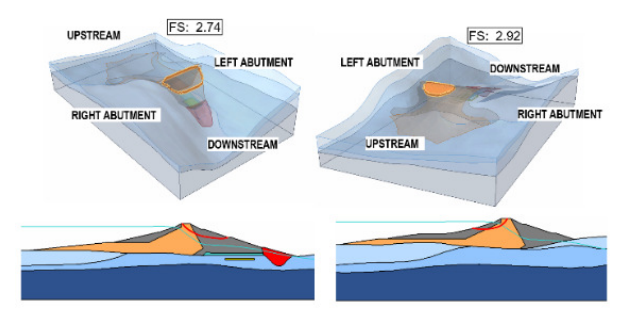


Figure 16. 3D stability analysis results - Static condition with reservoir at maximum level.

The summary of the safety factors obtained in both analyzes (2D and 3D), as well as a comparison of the differences between these methods, are presented in Table 5.

#### 4.4 Dynamic simulation results

#### 4.4.1 Simplified method

As a first approach to estimate earthquake-induced displacements for SEE Safety Evaluation Earthquake at the Quebradona dam, the Newmark (1965) model was used, using the approximate procedure developed by Makdisi and Seed (1978). For the development of the Makdisi and Seed iterative procedure, a value of PGA = 0.31g was adopted, upstream and downstream embankment height of 25 m and 34 m respectively, a maximum shear modulus value of 131 MPa, Vmax = 250 m/s and density of dam earth fill equal to 2000 kg/m³.

The results with this simplified methodology showed that the La Unión earthquake ground motion is the one that produces the largest displacements in the crest with 38 cm, followed by the Zihuatanejo ground motion with 22 cm and the Iwate earthquake with 4.0 cm. Therefore, nonlinear dynamic analyzes using the two-dimensional finite difference model described below were performed for these three input ground motions.

#### 4.4.2 Two-dimensional finite difference model

The two-dimensional numerical model for the non-linear dynamic analyzes started from a state of stress and pore pressures that approximates the current condition of the dam with the level of the reservoir at maximum (EL. 2095 masl). This stresses state was achieved through a steady flow analysis and a gravity loading stage that balances both the body forces and the pore pressure field using the Mohr-Coulomb model.

Prior to the dynamic analyzes the constitutive models were changed, using the PM4Silt model for the sandy silt and sandy fill of the dam body, the PM4Sand model for the foundation material corresponding to the alluvial deposit, saprolite (IC) and for the loose alluvial sand, the Mohr-Coulomb model with hysteretic damping in the draining blanket and the fill at the foot of the dam, and finally the linear elastic model for the rock basement.

Before the estimation of seismic induced deformation, the numerical model was calibrated to match the fundamental period of the dam estimated through the analysis of the ground motions recorded by the dam's accelerographs, which suggest a fundamental period of 0.32~s~(3.1~Hz). For this calibration, dynamic analyzes were carried out for a ground motion with an approximate duration of 5.0~s~ and a maximum acceleration of 0.02~ m/s², corresponding to the maximum acceleration recorded by the accelerograph located in rock and with which the fundamental period of the dam was obtained. With these results, the transfer function between the Fourier spectrum of the horizontal acceleration ground motion at the crest and the horizontal acceleration ground motion at the base of the model (input) was calculated.

Because the main factors that affect the fundamental period of the model are the geometry and the stiffness, this calibration procedure was carried out for the three-dimensional model, which considers the real geometry of the dam abutments and shape of canyon, adjusting the shear modulus coefficient G<sub>0</sub> that controls



the potential variation of the maximum shear modulus with the confinement of the different materials. Figure 17 shows the maximum shear modulus contours for the calibrated parameters and Figure 18 shows the transfer function for this two-dimensional model, indicating a fundamental period of 0.39 s, which, although greater than the fundamental period estimated with the instrumentation, it is considered suitable for two-dimensional analyzes due to the flat deformation condition of this model.

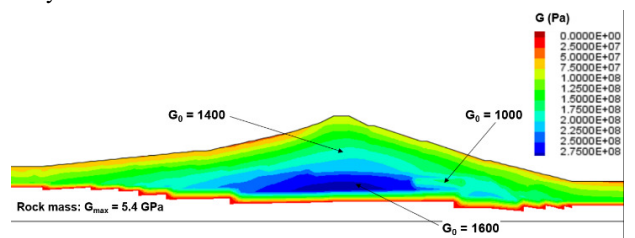


Figure 17. Calibrated maximum shear modulus - 2D FD model.

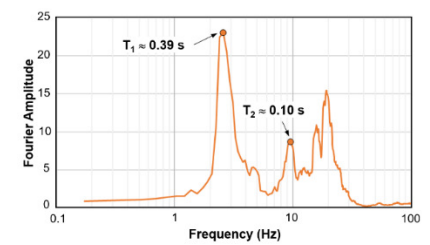


Figure 18. Transfer function - 2D FD model.

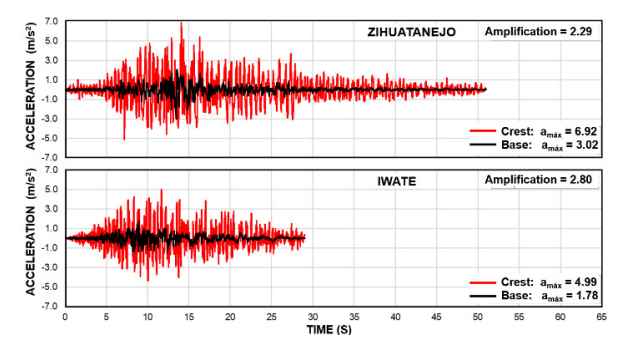


Figure 19. Horizontal acceleration (perpendicular to the dam axis) at the crest and base of the model - 2D Analysis.

Figure 19 illustrates the propagation of the seismic ground motion across the dam by showing the acceleration over time in a direction perpendicular to the dam's axis (x-direction in the numerical model). It presents data from two different analysis ground motions for two specific nodes: one on the dam's crest and another at the base of the model. The maximum recorded acceleration at the crest reached 6.92 m/s² for the Zihuatanejo input motion and 4.99 m/s² for the Iwate cortical input motion. These values represent amplification factors of 2.29 and 2.80, respectively.

The result of the nonlinear dynamic analysis in terms of the excess pore pressure and shear deformations at the end of the earthquake are presented in Figure 20 for the Zihuatanejo's ground motion. These results show that the highest pore pressures are generated in the loose alluvial sand and in the foundation both downstream and upstream, which correspond to the saturated

zones with lower confinements. As for shear deformations, the greatest strains reach up to 8% in the sand loose alluvial and deformations in the dam body range between 2% in the lower part to 5% at the crest of the dam. This magnitude of shear deformations can cause cracking in these sandy silt materials, which can generate internal erosion problems due to absence of adequate drainage elements in the dam.

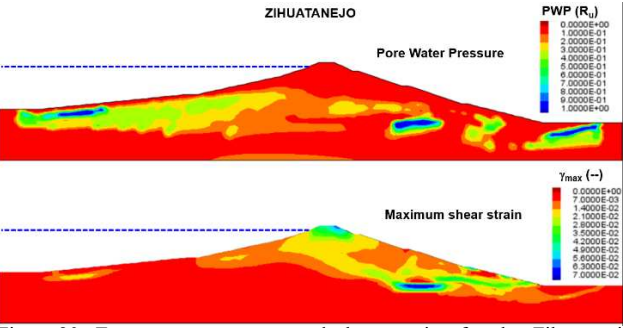


Figure 20. Excess pore pressure and shear strains for the Zihuatanejo earthquake after dynamic analysis - 2D FD model.

## 4.4.3 Three-dimensional finite difference model

Similar to 2D model, the three-dimensional numerical model for nonlinear dynamic analysis started from a state of stress and pore pressures that approximates the current state of the dam with reservoir at maximum level; this state of stress was achieved through the steady state flow analysis presented previously and a gravity loading stage that balances both the body forces and the pore pressure field using the Mohr-Coulomb constitutive model.

Prior to the dynamic analysis, the constitutive models of the materials were changed, using the P2PSand model for the materials of the embankment dam and its foundation with the exception of the filter and Rip-Rap, which were simulated with the Mohr Coulomb model with hysteretic damping, and the rock mass, for which the linear elastic model was used.

As mentioned above, the fundamental period of the three-dimensional finite difference model was calibrated so that the period calculated by the transfer function of a dynamic analysis coincided with the fundamental period measured by the dam's accelerographs. For this calibration, the shear modulus coefficient  $G_0$  of 1150 estimated for the body of the dam through the geophysical tests (MASW and SCPTu) and a  $G_0$  of 1400 for the foundation materials (IB and IC) were initially considered. These parameters were varied until the model period was adjusted. Figure 21 shows the transfer functions obtained from the dynamic analysis.

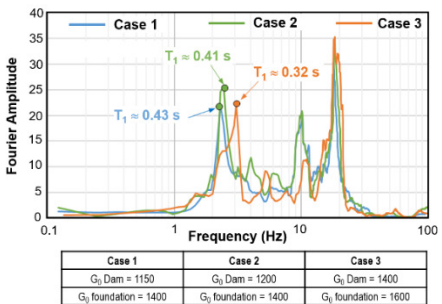


Figure 21. Transfer function-G0 calibration-2D FD model.



As seen in the previous figure for Case 3, corresponding to a parameter  $G_0$  of 1400 in the body of the dam and 1600 in the foundation, a fundamental period of 0.32 s is obtained, which coincides with the period measured by the instrumentation.

The non-linear dynamic analysis with the three-dimensional model was carried out for the ground motion that produces the largest settlements in the 2D model, the Zihuatanejo subduction ground motion. The pore pressure contours after the dynamic analysis in the 3D model are shown in Figure 22.

Compared to the initial pressures, a significant increase was observed in the loose alluvial sand and the upstream shoulder, zones with the minor effective stresses. These increases in pore pressure show the capabilities of the constitutive models used to produce volumetric deformations due to cyclic shear loads and the subsequent generation of pore pressure, which is essential because the materials of the body of the dam and its foundation may exhibit cyclic softening due to excessive deformation or liquefaction during rapid loading such as an earthquake.

Figure 23 shows the shear deformations resulting from dynamic analysis with the Zihuatanejo input motion in the three-dimensional model. Unlike the results of the two-dimensional model, in 3D model the greatest shear deformations occur superficially in the upstream shoulder, due to the greatest accelerations occurring in this superficial area, added to the lower rigidity materials of the upstream shoulder due to low effective stresses.

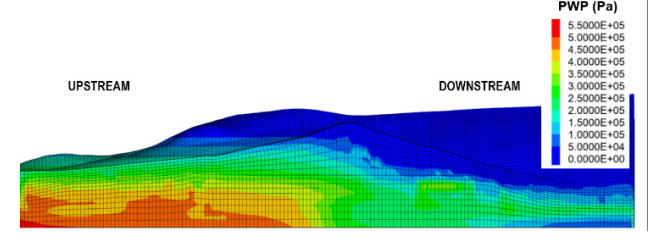


Figure 22. Excess pore pressure under the Zihuatanejo earthquake at the end of the dynamic analysis - 3D FD model

One of the main differences between the results of the twodimensional and three-dimensional model, which can be seen in Figure 23, is the lower shear deformation in the downstream shoulder in the 3D model, due to the stabilizing effect of the narrow canyon that considerably limits deformation of the loose alluvial sand layer. This effect was also seen in the three-dimensional limit equilibrium analyses, where the geometry of the downstream shoulder means the minimum failure surfaces do not deepen to the loose sand. These differences between the 2D and 3D model results are seen more clearly in Figure 25, which displays the magnitude of displacement in the maximum section of the dam is presented.

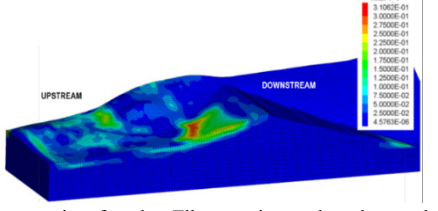


Figure 23. Shear strains for the Zihuatanejo earthquake at the end of the dynamic analysis - 3D FD model.

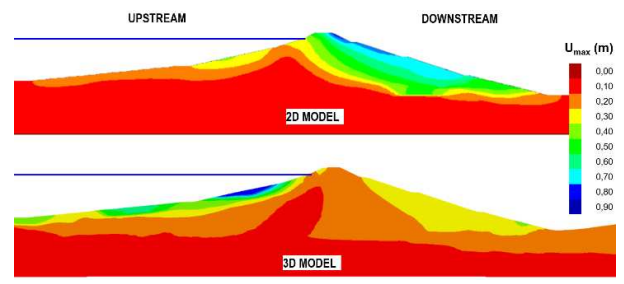


Figure 24. Comparison of total seismic displacements of 2D and 3D model after the earthquake in the maximum section of the dam

Evolution of crest settlements over time using the Zihuatanejo ground motion are presented in Figure 25, for both the two and three-dimensional dynamic analysis. This figure shows that although the three-dimensional model generates greater amplification of the seismic ground motion at the crest, the settlements at this point are less than half of those obtained in the 2D model, which is attributed to the more stable configuration of the three-dimensional model.

Based on the results obtained, it is concluded that in the event of the SEE safety evaluation earthquake, the settlement on the crest would be less than 60 cm, which can be safely absorbed by the current freeboard of 2.6 m.

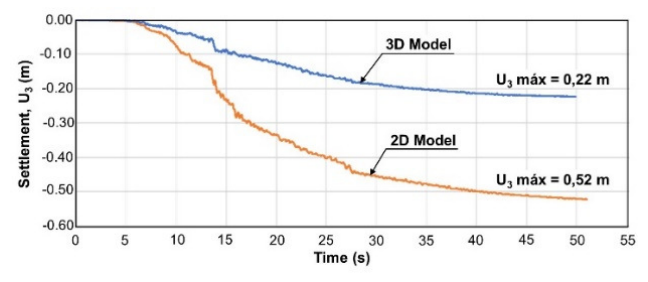


Figure 25. Settlement of the dam crest for Zihuatanejo earthquake - Finite difference model comparison, for two and three dimensions.

#### 5 DISCUSSIONS

The cyclic softening analyses results show that although the upstream and central fill of Quebradona dam is generally a silty sand, the high content of fines means this material behaves more as a fine material than a clayey silt. Therefore, the methodologies of Boulanger and Idriss (2014) and Kayen et al (2013) to evaluate the liquefaction potential are not appropriate since these were developed based on data that do not represent the behavior of the sandy silt of the dam. On the contrary, Robertson's (2009) methodology, which evaluates the possible cyclic softening of this material, shows satisfactory safety factors.

The crest accelerations results obtained are within expected values, with higher amplification factors when maximum acceleration of the input ground motion is lower, as in the Iwate earthquake. This behavior is due to the hysteretic damping presented by the constitutive models used for each of the zones and which guarantee a higher level of damping when the shear deformations are greater.

Liquefaction of the loose alluvial sand layer produces a surface of weakness, significant deformations in the dam body, and Proceedings of the 17<sup>th</sup> Pan-American Conference on Soil Mechanics and Geotechnical Engineering (XVII PCSMGE), and 2<sup>nd</sup> Latin-American Regional Conference of the International Association for Engineering Geology and the Environment (IAEG), La Serena Chile, 2024.

considerable movement of the downstream shoulder. The limit equilibrium stability showed that the downstream shell presents an important three-dimensional effect due to the narrow canyon. The slight curve at the rip-rap level and the loose sand stratum confinement generates a more stable configuration than that represented by a two-dimensional model.

#### 6 CONCLUSIONS

The geotechnical analysis models consider the presence of a sand lens in the dam foundation, which according to explorations carried out in 2007 is a material characterized as a fine saturated sand of low resistance and is susceptible to liquefaction phenomena. The complementary geotechnical exploration carried out for the present study made it possible to limit the spatial distribution of the loose sandy stratum.

The materials of the dam and its foundation have the capacity to generate excess pore pressure during a rapid load such as an earthquake, which can cause softening due to deformation or liquefaction of these materials, the latter mainly for the stratum of loose alluvial sand identified in the foundation.

Based on the characterization of the dam body, particularly the results of the SCPTu tests, the behavior of the dam under dynamic stress corresponds to a material with intermediate behavior between sand and clay with a tendency to dilatancy during shear, which has low susceptibility to liquefaction phenomena, but can present cyclic softening under seismic loads. These two phenomena (cyclic softening and susceptibility to liquefaction of the loose sand lens) have been accounted for in the numerical modeling through the selected constitutive models.

Crest settlements estimated with the two-dimensional and threedimensional finite difference models imply no problems of loss of free board that would affect safety of the dam in the event of an earthquake of significant magnitude, such as the SEE safety verification earthquake. While no significant seismic risk due to loss of free edge is identified in the Quebradona dam, shear deformations expected in the dam body of around 2% and greater than 5% in the crest of the dam imply high risk of cracking. Therefore, a recommendation was provided to protect the downstream shell of the dam with a filter blanket following the current state of practice for filter design.

#### 7 ACKNOWLEDGEMENTS

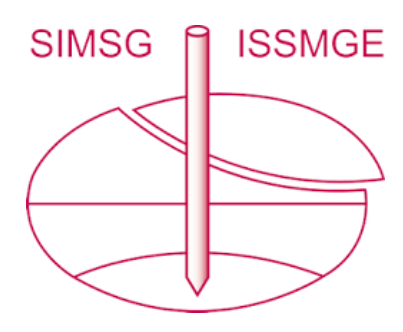
The authors express our gratefulness to EPM owner of Quebradona Dam and all the staff from the Dam Safety unit for its support during this study and for granting permission to publish this article.

#### 8 REFERENCES

- Abrahamson, N.A., Silva, W.J. and Kamai, R. 2014. Summary of the ASK14 Ground-Motion Relation for Active Crustal Regions. Earthquake Spectra Vol 30, Issue 3
- Atkinson G.M. and Boore D.M. 2003. Empirical ground-motion relations for the subduction-zone earthquakes and their application to Cascadia and other regions. *Bulletin of the Seismological Society of America*.
- Boulanger, R. W., and Idriss, I. M. 2014. CPT and SPT based liquefaction triggering procedures. Report No. UCD/CGM-14/01, Center for

- Geotechnical Modeling. Department of Civil and Environmental Engineering, University of California, Davis, CA, 134 pp
- Boulanger, R. W., and Ziotopoulou, K. 2017. "PM4Sand (version 3.1): A sand plasticity model for earthquake engineering applications." Report No. UCD/CGM-17/01, Center for Geotechnical Modeling, Department of Civil and Environmental Engineering, University of California, Davis, CA, March, 112 pp.
- Bray and Sancio. 2006. Assessment of the Liquefaction Susceptibility of Fine-Grained Soils. *Journal of Geotechnical and Geoenvironmental Engineering* 1 132(9). September 2006.
- Campbell K.W. and Bozorgnia Y. 2014. NGA-West2 Ground Motion Model for the Average Horizontal Components of PGA, PGV and 5% Damped Linear Acceleration Response Spectra. Earthquake Spectra.
- Cheng, Z. and Detournay D. 2021. Formulation, validation, and application of a practice-oriented two-surface plasticity sand model. *Computers and Geotechnics*, 132(4).
- Chiou B. and Youngs R. 2014. Update of the Chiou and Youngs NGA Model for the Average Horizontal Component of Peak Ground Motion and Response Spectra. Earthquake Spectra.
- Darendeli, M. B. 2001. Development of a New Family of Normalized Modulus Reduction and Material Damping Curves, Department of Civil, Architectural and Environmental Engineering, The University of Texas, Austin, Texas
- Idriss, I.M., and Boulanger, R.W. 2008. Soil liquefaction during earthquakes. Monograph MNO-12, Earthquake Engineering Research Institute. Oakland. CA
- Kayen R., Moss R.E.S., Thompson E.M., Seed R.B., Cetin K.O., Kiureghian A.Der., Tanaka Y. and Tokimatsu K. 2013. Shear-Wave Velocity Based Probabilistic and Deterministic Assessment of Seismic Soil Liquefaction Potential. *Journal of Geotechnical and Geoenvironmental Engineering*, 139:40719
- Makdisi, F. and Seed, H. 1978. Simplified procedure for estimating dam and embankment earthquake-induced deformations. *Journal of Geotechnical Engineering* 104(7): 849–867.
- Marulanda, A., Marulanda, C. and Hinks, J. 2023. Earthquake Engineering for Dams and Reservoirs. *Chapter 7 Seismic design of rockfill dams*. 65-103. Emerald Publishing Limited.
- Newmark, N. M. 1965. Effects of Earthquakes on Dams and Embankments, Geothecnique, London, England, Vol. 5, No. 2.
- Petersen, Mark & Moschetti, Morgan & Powers, et al. 2015. The 2014 United States National Seismic Hazard Model. Earthquake Spectra. 31. 10.1193/120814EQS210M.
- Robertson, P.K. 2009. Performance based earthquake design using the CPT. Proceedings of the International Conference on Performance-Based Design in Earthquake Geotechnical Engineering (IS-TOKYO 2009), 15-18
- Seed, H.B. and Idriss, I.M. 1970. Soil Moduli and Damping Factors for Dynamic Response Analyses. Report EERC 70-10. University of California-Berkeley.
- Youngs R. R., Chiou S. J., Silva W. J. and Humphrey J. R. 1997. Strong Ground Motion Attenuation Relationships for Subduction Zone Earthquakes, Seismological Research Letters, Vol. 68, No. 1, 58-73.
- Zhao, J. et al. 2006. Attenuation Relations of Strong Ground Motion in Japan Using Site Classification Based on Predominant Period, Bull. Seism. Soc. Am. 96, 898-913.

# INTERNATIONAL SOCIETY FOR SOIL MECHANICS AND GEOTECHNICAL ENGINEERING



This paper was downloaded from the Online Library of the International Society for Soil Mechanics and Geotechnical Engineering (ISSMGE). The library is available here:

# https://www.issmge.org/publications/online-library

This is an open-access database that archives thousands of papers published under the Auspices of the ISSMGE and maintained by the Innovation and Development Committee of ISSMGE.

The paper was published in the proceedings of the 17th Pan-American Conference on Soil Mechanics and Geotechnical Engineering (XVII PCSMGE) and was edited by Gonzalo Montalva, Daniel Pollak, Claudio Roman and Luis Valenzuela. The conference was held from November 12<sup>th</sup> to November 16<sup>th</sup> 2024 in Chile.